Research Square

Preprints are preliminary reports that have not undergone peer review.
They should not be considered conclusive, used to inform clinical practice,
or referenced by the media as validated information.

Winding-number staircase of the effective Lorentz factor and an analogue horizon in a ^{87}Rb ring Bose–Einstein condensate: two Bragg-resolvable predictions and a switched-shell null test

HASAN BÖREKCI

hborekci@hotmail.com.tr

HB ZECHMANN Medical Company https://orcid.org/0000-0001-9137-6342

Research Article

Keywords: analogue gravity, Bose–Einstein condensate, persistent current, sonic horizon, Bragg spectroscopy, ring trap

Posted Date: November 11th, 2026

DOI: https://doi.org/10.21203/rs.3.rs-11685117/v1

License: This work is licensed under a Creative Commons Attribution 4.0 International License.
Read Full License

Additional Declarations: The authors declare no competing interests.

Winding-number staircase of the effective Lorentz factor and an analogue horizon in a ^{87}Rb ring Bose–Einstein condensate: two Bragg-resolvable predictions and a switched-shell null test

Hasan Börekci

R&D Director, HB ZECHMANN Medical Company, Manisa Technopark, Manisa, Türkiye; independent theoretical physics researcher.

Correspondence: hborekci@hotmail.com.tr — ORCID: 0000-0001-9137-6342

Abstract

Persistent currents in ring-shaped Bose–Einstein condensates are quantised: the azimuthal flow speed can take only the discrete values $v = N\hbar/(mR)$ set by the winding number N. We point out that this turns the approach to the sonic (analogue-gravity) horizon into a reproducible staircase: in a ring of radius R = 20 μm with Bogoliubov sound speed c_s = 1.0 mm/s (peak density $n_0 \approx 2.8\times10^{13}$ cm^{-3}), one circulation quantum corresponds to $\Delta v \approx 36.5$ μm/s, the effective Lorentz factor of the phonon metric, $\gamma_{eff} = [1 - (v/c_s)^2]^{(-1/2)}$, climbs in discrete steps — 1.46 at N = 20, 2.46 at N = 25, 6.1 at N = 27 — and the first supersonic step, N = 28, creates an analogue horizon on the ring. We derive two quantitative, Bragg-resolvable predictions: (i) the step-resolved staircase of γ_{eff} itself, scanned reproducibly by preparing successive winding numbers, and (ii) a splitting $\Delta f = v/(\pi R)$ between co- and counter-propagating phonon modes — 15.7 Hz at N = 27, approaching 15.9 Hz as $v \to c_s$ — an analogue of frame dragging that extends to the horizon the Doppler readout of persistent currents already demonstrated at low winding number. Both are accessible to established mode-resolved phonon spectroscopy. We compare the ring-BEC platform with a superfluid ^{4}He giant-vortex alternative, and we propose a low-cost null test in which a macroscopic switchable current shell (kV–MV class) surrounds the shielded cell and is modulated 1 min ON / 1 min OFF: square-wave demodulation of Δf over one day bounds any anomalous fractional response at $|\delta\Delta f|/\Delta f < 1.5\times10^{-3}$ (1σ), improving as $1/\sqrt{\tau}$. The experiment is table-top scale and uses only established techniques.

Keywords: analogue gravity; Bose–Einstein condensate; persistent current; sonic horizon; Bragg spectroscopy; ring trap

1. Introduction

Analogue gravity rests on Unruh's observation that long-wavelength excitations of a moving medium propagate exactly as a massless field on an effective curved spacetime whose metric is built from the flow velocity and the medium's sound speed [1–3]. Where the flow becomes supersonic, the analogue of an event horizon forms. Bose–Einstein condensates (BECs) have become the leading platform for this programme [4–6]: stimulated and spontaneous analogue Hawking radiation have been reported in elongated condensates [7–10], and related analogue phenomena have been studied in water tanks [11], expanding condensates [12], and optical media [13].

In almost all of these experiments the flow profile is engineered hydrodynamically and varies continuously. Ring-shaped condensates offer a qualitatively different handle. In a multiply connected geometry the circulation is topologically quantised [14–17]: the azimuthal flow speed can take only the discrete values

$$v = N \hbar/(m R), \quad N = 0, 1, 2, \ldots$$

where m is the atomic mass and R the ring radius. Persistent currents with well-defined winding numbers have been created, stored and manipulated in ^{87}Rb rings for more than a decade — by phase imprinting and by stirring with rotating weak links — including deterministic preparation of high winding numbers and controlled single-quantum steps [14–17].

The simple point of this paper is that circulation quantisation converts the approach to the sonic horizon into a staircase. The control parameter of analogue-gravity experiments, the Mach number v/c_s, ceases to be a continuously tuned quantity and becomes a discrete, exactly reproducible one. Each step N is a distinct, re-preparable laboratory setting; the effective Lorentz factor of the phonon metric climbs step by step; and the horizon is reached not asymptotically but at a definite integer N_h. To our knowledge the staircase structure of the effective Lorentz factor, and its use as a calibration ladder for ring-based analogue-gravity measurements, have not been laid out quantitatively before.

We work throughout with one concrete design — a shielded, all-optical ^{87}Rb ring of radius R = 20 μm with design sound speed c_s = 1.0 mm/s — and derive two predictions accessible to mode-resolved phonon spectroscopy — Bragg spectroscopy [18] or in-situ Doppler readout of ring phonons [19]: the γ_eff staircase itself (Sec. 4.1) and a co-/counter-propagating phonon-mode splitting $\Delta f = v/(\pi R)$, 15.7 Hz at the last subsonic step and 15.9 Hz in the limit $v \to c_s$ (Sec. 4.2), the ring analogue of frame dragging. Section 5 compares the platform with a superfluid ^{4}He giant-vortex alternative [20,21]. Section 6 adds a methodological proposal: because the module is small, sealed and heavily shielded, it can be surrounded by a macroscopic switchable current shell and operated as a lock-in null test for any anomalous coupling between a switched electromagnetic energy flow and the analogue metric, with a model-independent one-day sensitivity of $|\delta\Delta f|/\Delta f < 1.5\times10^{-3}$.

A remark on origin, for transparency: this module was first designed by the author as a diagnostic channel inside a proposed large engineered-spacetime test apparatus [22,23]. The present paper extracts the module as a standalone, fully conventional analogue-gravity experiment; nothing in the predictions of Secs. 3–6 depends on that programme, and all numbers follow from standard Gross–Pitaevskii/Bogoliubov theory.

2. The system: a shielded ring condensate with a weak link

Figure 1 shows the module schematically, and Figure 2 shows conceptual three-dimensional renderings of the same design from four directions, with cutaways and a close-up of the cell region. A ^{87}Rb condensate of ~10^5 atoms is held in an all-optical ring trap of radius R = 20 μm inside an ultra-high-vacuum glass cell (10^{-11} mbar). The optical (rather than magnetic) trap allows the m_F = 0 state to be used and the whole cell to sit inside two nested μ-metal shields and a superconducting Pb shield. The Pb shield is held below its 7.2 K transition on the cold stage of an annular cryostat (with a copper radiation shield) whose room-temperature bore houses the cell, so the cell itself is never cooled. The stack rests on passive vibration isolation, light and control signals enter by fibre feedthroughs, and an ion pump outside the shields holds the vacuum through a CF40 port. A focused blue-detuned beam forms a rotating weak link (a stirring barrier) of the type used at

NIST to drive and read out persistent currents [16,17]; phase imprinting is an alternative preparation route [15].

The design parameters are collected in Table 1. With a_s = 5.3 nm for ^{87}Rb, the design sound speed c_s = (g n_0/m)^(1/2) = 1.0 mm/s corresponds to a peak density $n_0 \approx 2.8\times10^{13}$ cm^{-3} (Fig. 4b); a denser cloud, $n_0 = 10^{14}$ cm^{-3}, would give c_s = 1.9 mm/s, and every winding-number landmark below simply rescales with c_s. The healing length at the design density is ξ_h ≈ 0.52 μm, so R/ξ_h ≈ 39 and the azimuthal excitations of interest are safely hydrodynamic.

Parameter	Design value	Note
Ring radius R	20 μm	all-optical trap
Atom number	~10^5	^{87}Rb, m_F = 0
s-wave scattering length a_s	5.3 nm	≈100 a_0
Peak density n_0	2.8×10^{13} cm^{-3}	sets c_s = 1.0 mm/s
Sound speed c_s	1.0 mm/s	Bogoliubov, Fig. 4b
Healing length ξ_h	0.52 μm	R/ξ_h ≈ 39
Circulation quantum Δv = ħ/(mR)	36.5 μm/s	one winding step
Horizon winding number N_h = c_s mR/ħ	27.4	first supersonic step N = 28
Mode splitting at v = c_s, Δf = c_s/(πR)	15.9 Hz	15.7 Hz at N = 27

Table 1. Design parameters of the ring module.

Figure 1. Schematic cross-section of the shielded ^{87}Rb ring-BEC module: nested shields, UHV glass cell, all-optical ring trap with rotating weak link, and fibre feedthroughs. The headline numbers v = Nħ/(mR), Δv ≈ 36.5 μm/s and Δf ≈ 15.9 Hz are indicated.

Figure 2. Conceptual photorealistic renderings of the module — computer-generated design visualisations, not photographs of an existing apparatus; dimensions indicative. Cutaway views: (a) front, (b) side, (c) top, with lids and overhead imaging optics removed, (d) isometric, with (e) a close-up of the cell region. Beam colours are schematic and the ring BEC is drawn about 200× enlarged. 1 vibration-isolated optical table; 2 outer μ-metal shield; 3 inner μ-metal shield; 4 annular cryostat with copper radiation shield and superconducting Pb shield; 5 UHV glass cell; 6 ring BEC; 7 imaging/ring-trap objective; 8 Bragg-beam fibre collimators; 9 optical fibres through shield feedthroughs; 10 ion pump on CF40 port; 11 cryocooler; 12 imaging camera; 13 Bragg beams; 14 ring-trap and weak-link beams; 15 glass-to-metal transition and CF40 flange.

3. Effective metric and the quantised staircase

3.1 Phonon metric on the ring

In the hydrodynamic regime, phase fluctuations of the condensate obey a massless wave equation on the acoustic metric [1–4]

$$ds^2 \propto -(c_s^2 - v^2)\,dt^2 - 2\,v\,(R\,d\varphi)\,dt + (R\,d\varphi)^2 ,$$

written here for purely azimuthal flow of speed v on a thin ring; the radial and axial directions decouple for the lowest azimuthal branch. Two features of this metric drive everything below. First, the g_tφ cross term is proportional to v: a circulating flow drags phonons exactly as a rotating mass drags inertial frames in general relativity, so the ring realises a clean analogue of frame dragging (Sec. 4.2). Second, the g_tt coefficient

vanishes when v = c_s: the ergo/horizon condition on the ring. The natural measure of how close the flow is to this point is the effective Lorentz factor of the phonon metric,

$\gamma_{eff} = [1 - (v/c_s)^2]^{(-1/2)}$,

formally identical to the special-relativistic γ with c → c_s.

3.2 The staircase

Because v is quantised, γ_eff is quantised too. With the Table 1 parameters, one circulation quantum is $\Delta v = \hbar/(mR) = 36.5$ μm/s, and the horizon condition v = c_s falls at the non-integer winding number $N_h = c_s mR/\hbar = 27.4$; the last subsonic step is N = 27 and the first supersonic step is N = 28. Table 2 and Figure 3 give the staircase: γ_eff = 1.0007 at N = 1, 1.46 at N = 20, 2.46 at N = 25, 3.20 at N = 26, and 6.1 at N = 27; at N = 28 the counter-propagating phonon mode freezes and an analogue ergoregion/horizon is born on the ring. The Bogoliubov dispersion behind this picture, and the zero-frequency crossing of the counter-propagating branch that defines the horizon, are drawn in Figure 4a.

N (windings)	**v (mm/s)**	**v/c_s**	**γ_eff**
1	0.037	0.037	1.0007
5	0.183	0.183	1.017
10	0.365	0.365	1.074
15	0.548	0.548	1.196
20	0.731	0.731	1.465
25	0.913	0.913	2.457
26	0.950	0.950	3.201
27	0.986	0.986	6.105
28	1.023	1.023	horizon (supersonic)

Table 2. Quantised flow steps in the ^{87}Rb ring (R = 20 μm, c_s = 1.0 mm/s).

Three properties distinguish this staircase from a continuously tuned Mach number. (i) Reproducibility: each rung is a topologically protected laboratory setting; preparing "N = 25" twice gives the same v/c_s to the accuracy with which R and c_s are known, with no analogue in continuously stirred systems. (ii) Self-calibration: the ratio v/c_s = N/N_h involves a known integer and a single measured quantity N_h, so systematic errors in absolute calibrations of density or trap geometry largely cancel along the ladder. (iii) A sharp horizon onset: the horizon appears between two integers (here 27 and 28), so its signatures can be compared across a discrete jump rather than a gradual crossover.

Figure 3. Effective Lorentz factor versus flow: (a) the continuous relation with the quantised steps marked, and the analogue-horizon condition at v = c_s; (b) the same staircase versus winding number N, with N_h = 27.4 indicated.

Figure 4. (a) Bogoliubov dispersion in the flowing ring at v = 0.99 c_s (N = 27): co- and counter-propagating branches; for v > c_s the counter-propagating branch crosses zero frequency — the analogue-horizon condition. (b) The Bogoliubov sound speed $c_s = (g n_0/m)^{(1/2)}$ for ^{87}Rb; the design point c_s = 1.0 mm/s corresponds to $n_0 \approx 2.8\times10^{13}$ cm^{-3}.

4. Two Bragg-resolvable predictions

4.1 Step-resolved γ_eff

Mode-resolved phonon spectroscopy measures the frequency of a phonon mode of chosen wavenumber directly — by Bragg scattering [18] or, in ring condensates, by in-situ imaging of the precession of a standing-wave phonon [19]; in-situ density imaging is also the basis of the BEC analogue-Hawking measurements [8–10]. On the ring, the lowest azimuthal modes have wavenumber $k_j = j/R$ (integer j), i.e. frequencies of order $c_s/(2\pi R) \approx 8$ Hz and up. Preparing successive winding numbers N = 0, 5, 10, …, 27 and recording the mode frequencies maps the entire staircase of Table 2 in one apparatus; γ_eff at each rung follows from the measured co-/counter-propagating pair without any absolute density calibration (Sec. 4.2). The prediction is the full curve of Figure 3 — not a single point — which makes it an unusually stringent, over-constrained test of the acoustic-metric description in a multiply connected geometry.

4.2 Mode splitting: the ring analogue of frame dragging

For flow speed v, the lowest co- and counter-propagating azimuthal phonons are Doppler-split by

$$\Delta f = f_+ - f_- = 2 \cdot v\, k_1/(2\pi) = v/(\pi R),$$

the acoustic analogue of the Sagnac/Lense–Thirring splitting produced by the $g_{t\varphi}$ term. At the last subsonic step (N = 27, v = 0.987 c_s) this is $\Delta f \approx 15.7$ Hz for the Table 1 parameters, approaching $c_s/(\pi R) \approx 15.9$ Hz as $v \to c_s$ (Figure 5). The low-N end of this ladder is not hypothetical: the Doppler shift of azimuthal phonons by a persistent current has been measured in a ^{87}Rb ring and used to read out individual winding numbers in situ [19]. The new element here is to follow the same observable step by step up to the horizon. The splitting grows linearly along the staircase (0.58 Hz per winding step), so the Δf ladder and the γ_eff ladder are measured simultaneously from the same spectra: Δf fixes v, the mean frequency fixes c_s, and γ_eff follows with both systematics cancelling in the ratio.

Figure 5. Predicted Bragg spectrum of the lowest azimuthal mode pair at N = 27 (Lorentzian linewidths illustrative): the flow splits the co- and counter-propagating phonons by $\Delta f = v/(\pi R) \approx 15.7$ Hz (15.9 Hz in the limit $v \to c_s$).

5. Comparison with a superfluid ^{4}He giant vortex

The same staircase logic applies to any quantised superflow, and superfluid ^{4}He is the historical home of circulation quantisation and phase-slip physics [20,21]. A He-II "giant vortex" or annular flow offers robustness, large volumes and cryogenic simplicity, and its circulation quantum $\kappa = h/m_4$ is fixed by nature. For the present purpose, however, the ^{87}Rb ring has three decisive advantages. First, scale separation: in He-II the sound speed is ~240 m/s, so reaching $v \sim c_s$ in circulation-quantised flow would require astronomically high winding numbers, whereas the dilute BEC's millimetre-per-second c_s puts the horizon at $N_h \approx 27$. Second, diagnostics: in-situ imaging and Bragg spectroscopy give direct, mode-resolved access to the phonon field [18,19], with no cryogenic transducer chain. Third, tunability: density (hence c_s and N_h) is adjustable optically, allowing the staircase to be rescaled at will (Fig. 4b). The He-II route remains attractive as a complementary, materially independent check at a different point of parameter space, and nothing below depends on which platform is chosen.

6. A switched-shell null test

Because the module is sealed, shielded and table-top sized, it also lends itself to a clean methodological experiment: surround the shield stack with a macroscopic switchable current shell — a kV–MV-class electron-beam or current loop arrangement — and modulate it with a 1 min ON / 1 min OFF square wave, 720 cycles per day (Figure 6a). Standard physics predicts no effect of the shell on the phonon spectrum once ordinary electromagnetic pickup is excluded by the shields; the measurement therefore functions as a null test with a quantitative, model-independent sensitivity, in the spirit of lock-in searches for anomalous couplings.

The protocol discards the first 5 s after every switch (settling), leaving 55 usable seconds per half-cycle; with a 10 s preparation-and-probe cycle this yields 5 Bragg shots per window and 3600 shots per shell state per day. Operating at $N = 27$ ($\Delta f \approx 15.7$ Hz) and taking a conservative single-shot uncertainty of $\sigma_{shot} = 1$ Hz on Δf, the daily mean of each state carries $\sigma = 1\ \text{Hz}/\sqrt{3600} \approx 17$ mHz, and the ON−OFF difference is bounded at 1σ by $|\delta\Delta f| < \sqrt{2} \times 17\ \text{mHz} \approx 24$ mHz, i.e.

$|\delta\Delta f| / \Delta f < 1.5\times10^{-3}$ (one day), improving as $1/\sqrt{\tau}$ to 2.7×10^{-4} in 30 days (Figure 6b).

The same demodulation applied to the step positions (N_h) bounds anomalous shifts of c_s. We emphasise the honest framing: there is no standard-physics mechanism by which the shell, once screened, should move Δf at any detectable level; the value of the measurement is (i) as a stringent systematics audit of the platform itself, and (ii) as a cheap, quantitative constraint on any speculative proposal — including the author's own [22,23] — in which macroscopic electromagnetic energy flows are conjectured to deform the effective metric seen by laboratory probes. A null result is the expected outcome and is scientifically useful as such.

Figure 6. The switched-shell null test. (a) Geometry: the shielded ring-BEC cell inside a switchable kV–MV-class current shell, modulated 1 min ON / 1 min OFF. (b) 1σ bound on the fractional ON−OFF response of the mode splitting versus integration time: $|\delta\Delta f|/\Delta f < 1.5\times10^{-3}$ after one day, scaling as $1/\sqrt{\tau}$.

7. Feasibility and outlook

Every element of the proposal is established technology: optical ring traps and deterministic persistent-current preparation [14–17], weak-link stirring with single-quantum control [16,17], mode-resolved phonon spectroscopy with single-winding-number sensitivity [18,19], and magnetic/electrostatic shielding at the levels routinely used in precision atomic experiments. High winding numbers are the main experimental risk: $N \gtrsim 27$ in a 20 μm ring corresponds to $v \approx 1$ mm/s, comparable to flows already demonstrated in stirred rings, but step-by-step stability up to N_h, and controlled crossing of the first supersonic step, will need care with the weak-link ramp to avoid uncontrolled phase slips [16,20]. The reward is a discrete, self-calibrating analogue-gravity ladder: a staircase of effective Lorentz factors ending at a horizon whose onset lies between two integers, with both observables read from a single phonon spectrum. Natural extensions include thermometry of the mode pair across the $N = 27 \rightarrow 28$ jump (the analogue-Hawking channel studied in elongated systems [8–10], here with a topologically sharp onset) and the rescaling of the whole ladder by optical control of the density (Fig. 4b).

8. Conclusion

Circulation quantisation turns a ring-shaped ^{87}Rb condensate into a stepwise analogue-gravity laboratory. For a 20 μm ring at c_s = 1.0 mm/s: the effective Lorentz factor climbs a reproducible staircase ($\gamma_{eff} \approx 6.1$ at N = 27), an analogue horizon is born at the first supersonic step N = 28, and the co-/counter-propagating phonon splitting $\Delta f = v/(\pi R)$ (15.7 Hz at N = 27) provides a frame-dragging analogue — all accessible to established mode-resolved phonon spectroscopy, with the key systematics cancelling in ratios along the ladder. A switched-current-shell lock-in adds a model-independent null test at the 10^{-3}-per-day level. The experiment is table-top scale, uses only demonstrated techniques, and offers the analogue-gravity community a discrete calibration ladder that continuously stirred systems cannot provide.

Declarations

Funding and independence. Dr. Hasan Börekci received no institutional support for the design or writing of this work; he is not employed by any state-affiliated institution and produced this work with his own means. The conception, planning and apparatus design are his own. AI assistance (Claude, Anthropic) was used for the literature search, calculations and page layout, under the author's direction and verification.

Conflicts of interest. The author declares no conflict of interest.

Data availability. The calculation scripts reproducing every number and figure in this paper are available from the author on request.

References

[1] W. G. Unruh, "Experimental black-hole evaporation?", Phys. Rev. Lett. 46, 1351 (1981). DOI: 10.1103/PhysRevLett.46.1351

[2] M. Visser, "Acoustic black holes: horizons, ergospheres and Hawking radiation", Class. Quantum Grav. 15, 1767 (1998). DOI: 10.1088/0264-9381/15/6/024

[3] C. Barceló, S. Liberati and M. Visser, "Analogue gravity", Living Rev. Relativ. 14, 3 (2011). DOI: 10.12942/lrr-2011-3

[4] L. J. Garay, J. R. Anglin, J. I. Cirac and P. Zoller, "Sonic analog of gravitational black holes in Bose–Einstein condensates", Phys. Rev. Lett. 85, 4643 (2000). DOI: 10.1103/PhysRevLett.85.4643

[5] O. Lahav, A. Itah, A. Blumkin, C. Gordon, S. Rinott, A. Zayats and J. Steinhauer, "Realization of a sonic black hole analog in a Bose–Einstein condensate", Phys. Rev. Lett. 105, 240401 (2010). DOI: 10.1103/PhysRevLett.105.240401

[6] M. J. Jacquet, S. Weinfurtner and F. König, "The next generation of analogue gravity experiments", Phil. Trans. R. Soc. A 378, 20190239 (2020). DOI: 10.1098/rsta.2019.0239

[7] J. Steinhauer, "Observation of self-amplifying Hawking radiation in an analogue black-hole laser", Nat. Phys. 10, 864 (2014). DOI: 10.1038/nphys3104

[8] J. Steinhauer, "Observation of quantum Hawking radiation and its entanglement in an analogue black hole", Nat. Phys. 12, 959 (2016). DOI: 10.1038/nphys3863

[9] J. R. Muñoz de Nova, K. Golubkov, V. I. Kolobov and J. Steinhauer, "Observation of thermal Hawking radiation and its temperature in an analogue black hole", Nature 569, 688 (2019). DOI: 10.1038/s41586-019-1241-0

[10] V. I. Kolobov, K. Golubkov, J. R. Muñoz de Nova and J. Steinhauer, "Observation of stationary spontaneous Hawking radiation and the time evolution of an analogue black hole", Nat. Phys. 17, 362 (2021). DOI: 10.1038/s41567-020-01076-0

[11] S. Weinfurtner, E. W. Tedford, M. C. J. Penrice, W. G. Unruh and G. A. Lawrence, "Measurement of stimulated Hawking emission in an analogue system", Phys. Rev. Lett. 106, 021302 (2011). DOI: 10.1103/PhysRevLett.106.021302

[12] S. Eckel, A. Kumar, T. Jacobson, I. B. Spielman and G. K. Campbell, "A rapidly expanding Bose–Einstein condensate: an expanding universe in the lab", Phys. Rev. X 8, 021021 (2018). DOI: 10.1103/PhysRevX.8.021021

[13] U. Leonhardt and P. Piwnicki, "Relativistic effects of light in moving media with extremely low group velocity", Phys. Rev. Lett. 84, 822 (2000). DOI: 10.1103/PhysRevLett.84.822

[14] C. Ryu, M. F. Andersen, P. Cladé, V. Natarajan, K. Helmerson and W. D. Phillips, "Observation of persistent flow of a Bose–Einstein condensate in a toroidal trap", Phys. Rev. Lett. 99, 260401 (2007). DOI: 10.1103/PhysRevLett.99.260401

[15] A. Ramanathan, K. C. Wright, S. R. Muniz, M. Zelan, W. T. Hill III, C. J. Lobb, K. Helmerson, W. D. Phillips and G. K. Campbell, "Superflow in a toroidal Bose–Einstein condensate: an atom circuit with a tunable weak link", Phys. Rev. Lett. 106, 130401 (2011). DOI: 10.1103/PhysRevLett.106.130401

[16] K. C. Wright, R. B. Blakestad, C. J. Lobb, W. D. Phillips and G. K. Campbell, "Driving phase slips in a superfluid atom circuit with a rotating weak link", Phys. Rev. Lett. 110, 025302 (2013). DOI: 10.1103/PhysRevLett.110.025302

[17] S. Eckel, J. G. Lee, F. Jendrzejewski, N. Murray, C. W. Clark, C. J. Lobb, W. D. Phillips, M. Edwards and G. K. Campbell, "Hysteresis in a quantized superfluid atomtronic circuit", Nature 506, 200 (2014). DOI: 10.1038/nature12958

[18] J. Stenger, S. Inouye, A. P. Chikkatur, D. M. Stamper-Kurn, D. E. Pritchard and W. Ketterle, "Bragg spectroscopy of a Bose–Einstein condensate", Phys. Rev. Lett. 82, 4569 (1999). DOI: 10.1103/PhysRevLett.82.4569

[19] A. Kumar, N. Anderson, W. D. Phillips, S. Eckel, G. K. Campbell and S. Stringari, "Minimally destructive, Doppler measurement of a quantized flow in a ring-shaped Bose–Einstein condensate", New J. Phys. 18, 025001 (2016). DOI: 10.1088/1367-2630/18/2/025001

[20] O. Avenel and E. Varoquaux, "Observation of singly quantized dissipation events obeying the Josephson frequency relation in the critical flow of superfluid ⁴He through an aperture", Phys. Rev. Lett. 55, 2704 (1985). DOI: 10.1103/PhysRevLett.55.2704

[21] R. J. Donnelly, Quantized Vortices in Helium II (Cambridge University Press, Cambridge, 1991). ISBN 978-0-521-32400-7

[22] H. Börekci, "NEW.BEF: a triple-capsule near-light-speed enclosing energy-field apparatus — technical report (EN/TR) with calculation scripts", Zenodo (2026). DOI: 10.5281/zenodo.23272711

[23] H. Börekci, "A near-light-speed enclosing energy field as a positron source and candidate time-dilation capsule", Research Square preprint (2026). DOI: 10.21203/rs.3.rs-9999735/v1

Figures

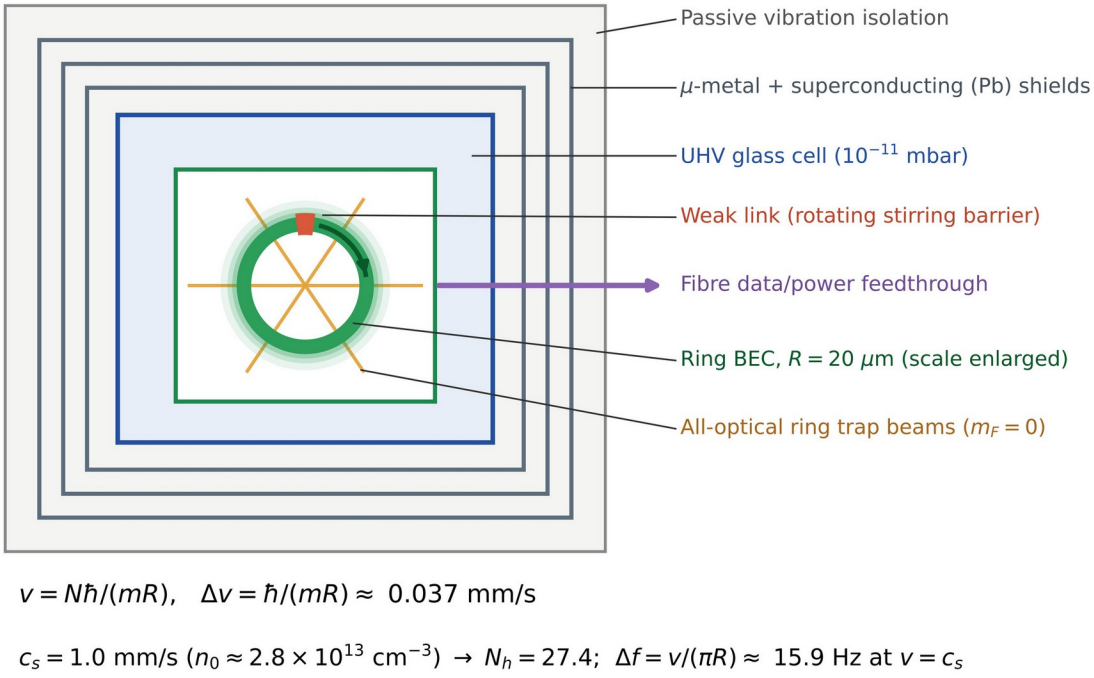


Figure 1. Schematic cross-section of the shielded ^{87}Rb ring-BEC module: nested shields, UHV glass cell, all-optical ring trap with rotating weak link, and fibre feedthroughs. The headline numbers v = Nh/(mR), Δv ≈ 36.5 μm/s and Δf ≈ 15.9 Hz are indicated.

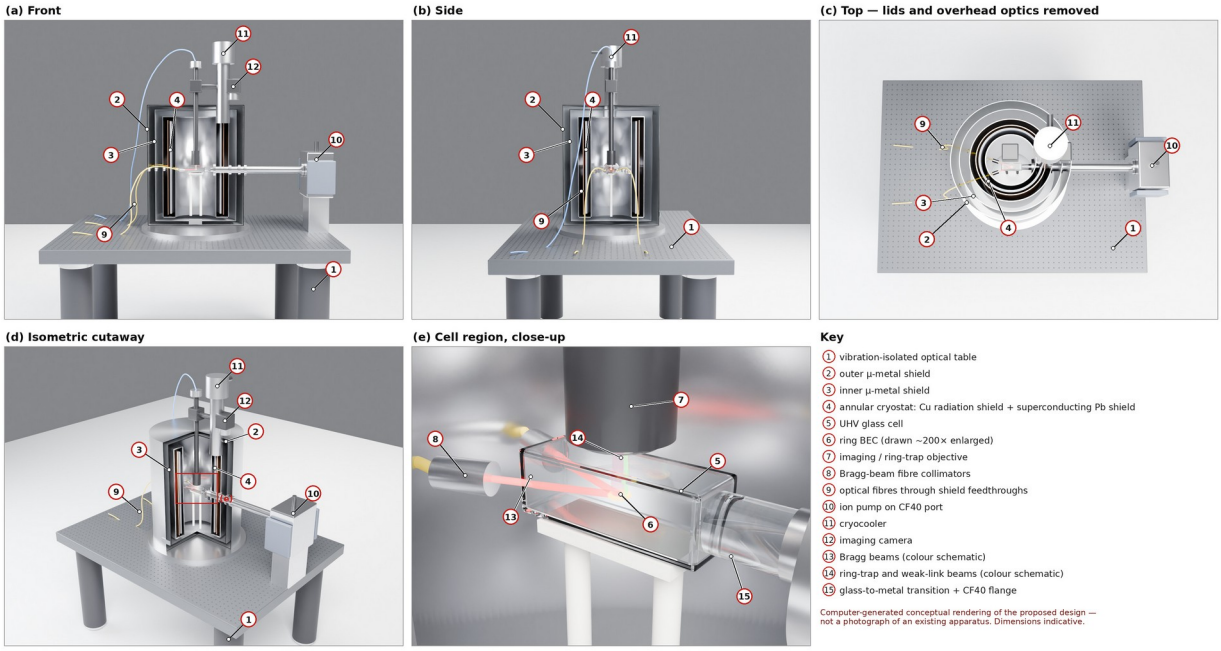


Figure 2. Conceptual photorealistic renderings of the module — computer-generated design visualisations, not photographs of an existing apparatus; dimensions indicative. Cutaway views: (a) front, (b) side, (c) top, with lids and overhead imaging optics removed, (d) isometric, with (e) a close-up of the cell region. Beam colours are schematic and the ring BEC is drawn about 200× enlarged. 1 vibration-isolated optical table; 2 outer μ-metal shield; 3 inner μ-metal shield; 4 annular cryostat with copper radiation shield and superconducting Pb shield; 5 UHV glass cell; 6 ring BEC; 7 imaging/ring-trap objective; 8 Bragg-beam fibre collimators; 9 optical fibres through shield feedthroughs; 10 ion pump on CF40 port; 11 cryocooler; 12 imaging camera; 13 Bragg beams; 14 ring-trap and weak-link beams; 15 glass-to-metal transition and CF40 flange.

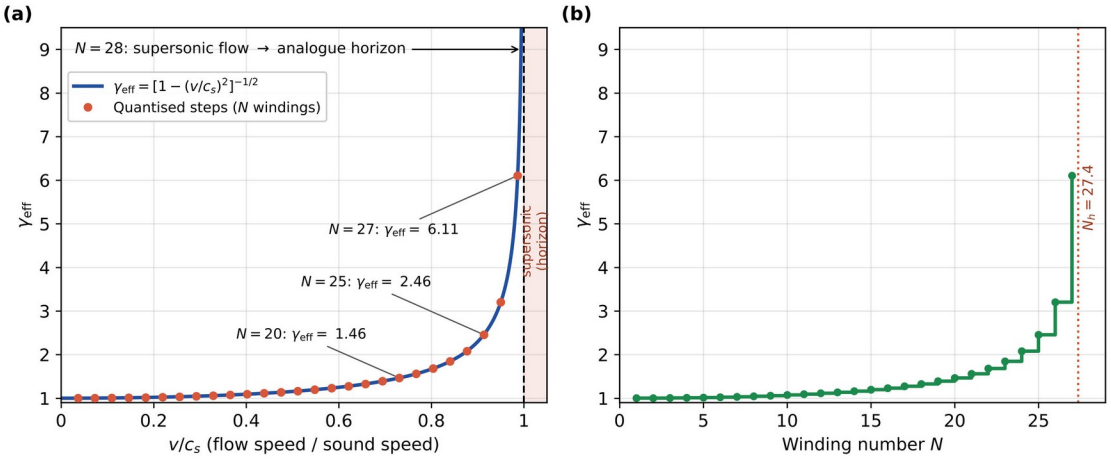


Figure 3. Effective Lorentz factor versus flow: (a) the continuous relation with the quantised steps marked, and the analogue-horizon condition at v = c_s; (b) the same staircase versus winding number N, with N_h = 27.4 indicated.

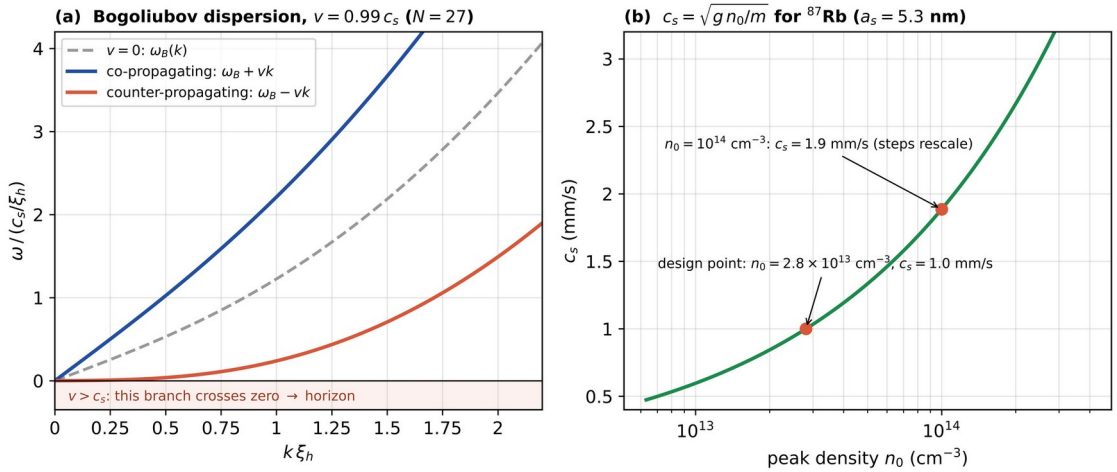


Figure 4. (a) Bogoliubov dispersion in the flowing ring at v = 0.99 c_s (N = 27): co- and counter-propagating branches; for v > c_s the counter-propagating branch crosses zero frequency — the analogue-horizon condition. (b) The Bogoliubov sound speed c_s = (g n$_0$/m)^(1/2) for ^{87}Rb; the design point c_s = 1.0 mm/s corresponds to n$_0$ ≈ 2.8×10¹³ cm⁻³.

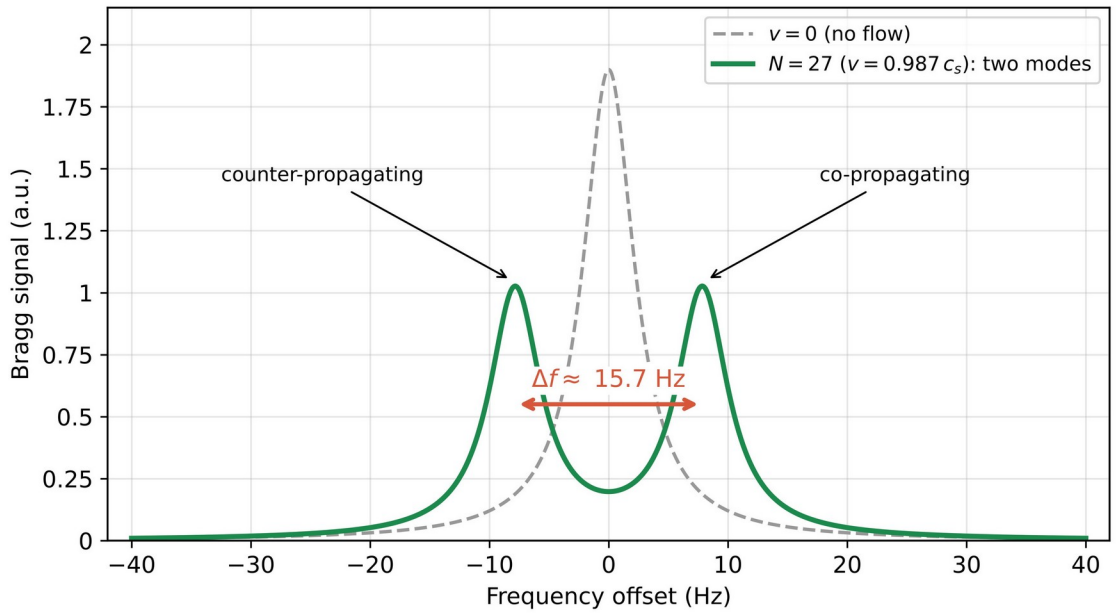


Figure 5. Predicted Bragg spectrum of the lowest azimuthal mode pair at N = 27 (Lorentzian linewidths illustrative): the flow splits the co- and counter-propagating phonons by Δf = v/(πR) ≈ 15.7 Hz (15.9 Hz in the limit v → c_s).

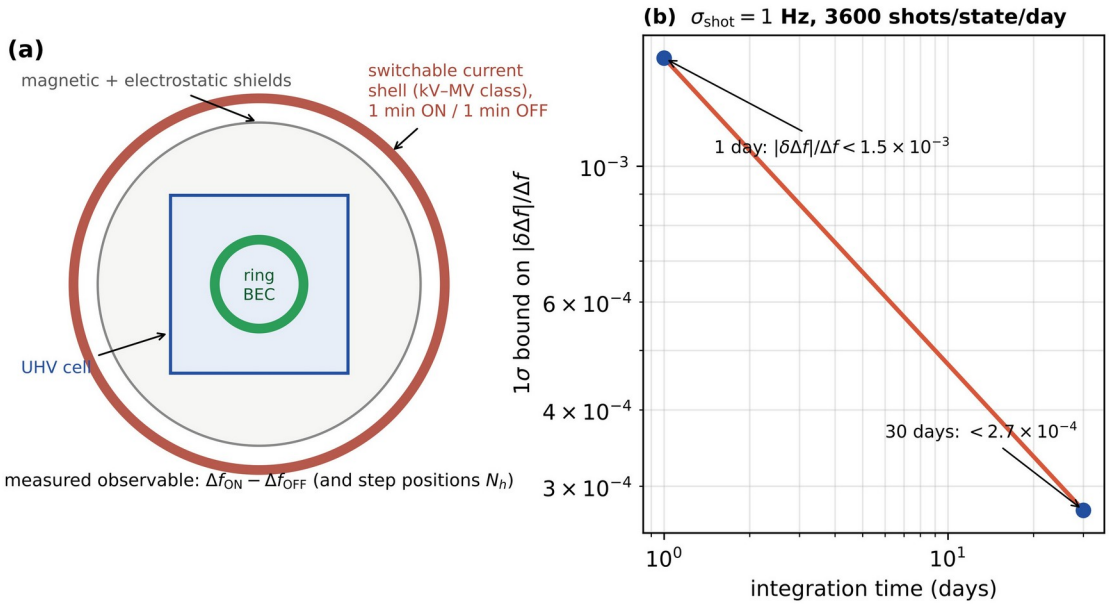


Figure 6. The switched-shell null test. (a) Geometry: the shielded ring-BEC cell inside a switchable kV–MV-class current shell, modulated 1 min ON / 1 min OFF. (b) 1σ bound on the fractional ON−OFF response of the mode splitting versus integration time: $|\delta\Delta f|/\Delta f < 1.5\times10^{-3}$ after one day, scaling as $1/\sqrt{\tau}$.